IEEE Access
Multidisciplinary | Rapid Review | Open Access Journal

Received December 30, 2017, accepted February 13, 2018, date of publication February 27, 2018, date of current version April 23, 2018.

Digital Object Identifier 10.1109/ACCESS.2018.2810128

Design and Optimization of Load-Independent Magnetic Resonant Wireless Charging System for Electric Vehicles

CHANGSONG CAI[1], (Student Member, IEEE), JUNHUA WANG[1], (Member, IEEE), ZHIJIAN FANG[1], PENGCHENG ZHANG[2,3], MEILIN HU[1], JUNKUN ZHANG[4], LIANG LI[1], AND ZHONGZHENG LIN[1]

[1]School of Electrical Engineering, Wuhan University, Wuhan 430072, China
[2]School of Electrical Engineering, Hebei University of Technology, Tianjin 300130, China
[3]School of Electrical and Computer Engineering, Georgia Institute of Technology, Atlanta, GA 30332, USA
[4]Institute of New Energy, Wuhan 430040, China

Corresponding author: Junhua Wang (junhuawang@whu.edu.cn)

This work was supported in part by the National Natural Science Foundation of China under Project 51707138 and Project 51507114 and in part by the National Key Research and Development Plan under Project 2017YFB1201002.

ABSTRACT A load-independent wireless power transfer system with constant current and constant voltage output for electric vehicles charging is designed and optimized in this paper. Wireless charging system based on *LCL*-S or *LCL–LCL* compensation topology is systematically analyzed. And dynamic *LCL*-S/*LCL* switching topology is designed and simplified to achieve constant current in the transmitting coil and load-independent constant current and constant voltage output, which can be controlled easily. Moreover, the coupling structures composed of different coil shapes and shielding structures are comparatively studied to improve the coupling stability under misalignment. Figure-of-merit and coupling change rate Δk_t defined in this paper are the key parameters in the process of coupling structure design and optimization. The combination of rounded rectangular spiral coil and splicing magnet core units is optimized as the coupling structure of the wireless charging system. Finally, the resonant wireless charging system prototype is being built and tested. The experimental results show that the load-independent and other characteristics of the implemented system are well correlated with the theoretical analysis and design.

INDEX TERMS Load-independent, wireless charging system, compensation topology, coupling structure.

I. INTRODUCTION

Wireless charging technology is more convenient and secure compared with traditional physical contact charging method. This novel and dominant power transmission mode has attracted more and more attention in the field of electric vehicles (EVs) and other charging applications. Especially when researchers at MIT proposed the magnetic resonance coupled wireless charging technology, it sets off a new chapter in this field [1]–[4]. The study of this technology applied for EVs charger is mainly focused on improving the transmission efficiency, increasing the transmission distance and ensuring the safety of electromagnetic environment [5]–[7].

It is desirable that the charging process of EVs is stable in practice. However, the equivalent resistance of lithium-ion batteries varies during charging process, and parking deviation of EVs causes variation of the coupling coefficient between the transmitter and receiver. Variations of equivalent resistance and coupling coefficient make changes in the equivalent reflected load parameters at the transmitter, and that may worsen charging quality. Moreover, the characteristics of lithium batteries need a constant current (CC) or constant voltage (CV) input [8], [9]. Therefore, it is necessary to design a stable load-independent wireless charging system with CC/CV output for EVs.

Compensation topology of resonant wireless charging system is used to make the transmitter and receiver in resonance to enhance its transmission performance. LCL topology has been considered as a desired resonant compensation used in the transmitter, which makes the current in transmitting coil independent from varying impedance with proper parameters design [10], [11]. However, making the current in transmitter constant is not enough to achieve a stable system performance, the coupling coefficient between transmitter and receiver is another key factor. Reference [12] analyzes

coupling characteristic of coils with different shapes. A wireless charging system was established with 21-cm-diameter coils, and coupling coefficient of the system is more than 0.2 when the distance is less than 8 cm. Reference [13] uses an optimized magnetic shield structure at both transmitting and receiving sides to achieve efficient power transmission, and the final 70-cm-diameter circular coupling structure was constructed and tested with good tolerance to misalignment at a distance of 13 cm. Reference [14] realizes optimum 88% transmission efficiency when the transmission power is 500 W at 15 cm distance based on mutual inductance coefficient optimization and frequency splitting avoidance. These studies all put emphasis on coupling enhancement with exclusion of complete and systematical analysis from influence of coil shape, winding layout and magnetic core placement on the system performance.

Furthermore, various methods have been studied to achieve the required CC or CV output under equivalent load variations of batteries. The primitive way to realize the CC/CV output is adding a conversion circuit at the primary or secondary side of the wireless charging system. Reference [15] designed a closed-loop wireless charging system with a charging information feeding-back route to the primary side in real time, and DC-DC converter is added at primary side to realize CC/CV output for charging. Reference [16] achieves stable CC/CV output when load changes by regulating the DC-DC converter at secondary side of the system. This method of converter addition increases energy loss and takes up more space. Reference [17] realizes constant current charging with SS/SP compensation structure and variable load with frequency adjustment. Due to effect neglect of load variation range in analysis process, the proposed method can only suit in a certain load range. In order to solve the shortcomings of those methods, [18] proposes a SS and PS or SP and PP switching topology system to implement CC/CV output with a constant frequency for batteries and the designed system can realize zero phase angle (ZPA) for pure resistance equivalent impedance. The topology in [18] has advantages in system simplicity and reliability, but it does exclude the influence of input misalignment from primary side on the performance.

According to the above studies, a stable load-independent wireless charging system with constant current or constant voltage output is designed and optimized in this paper. Load-independent, constant emission current and other characteristics of the wireless charging system with dynamic switching topology based on LCL-S compensation and LCL-LCL compensation respectively are all systematically analyzed and designed. Moreover, the coupling structures composed of different coils and shielding structures are comparatively studied to achieve a better misalignment tolerance. Figure-of-Merit (FOM) and coupling change rate Δk_t defined in this paper are key parameters in the process of coupling structure design and optimization. The combination of rounded rectangular spiral coil and splicing magnet core units is optimized as the coupling structure of the EVs wireless charging system, whose compensation topology is a dynamic LCL-S/LCL switching topology for load-independent CC/CV output. Finally, experiment verifies the system load-independent and its relative characteristics.

II. ANALYSIS AND DESIGN OF COMPENSATION TOPOLOGY

A. ANALYSIS OF LCL-S COMPENSATION TOPOLOGY

Due to the parking deviation and misalignment of EVs, LCL topology is designed as the compensation topology in the transmitter to make the current constant in transmitting coil even if the reflected impedance of receiver changes. The topology scheme of the LCL-S compensated wireless charging system is shown in Fig. 1.

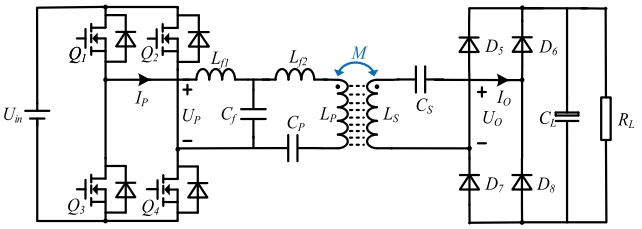

FIGURE 1. Converter circuit of LCL-S compensated wireless charging system.

L_P and L_S are the self-inductances of the transmitting and receiving coils, C_P and C_S are the compensation capacitors, M is the mutual-inductance between the transmitter and receiver. And the equivalent resistances of the coils are ignored. L_{f1}, L_{f2}, C_f are the resonant elements of LCL compensation topology in the transmitter. U_{in} is DC input of the convertor, and Q_1, Q_2, Q_3, Q_4 are switching modules of the H-bridge convertor. U_P and I_P are the high frequency output voltage and current of the convertor, U_O and I_O is the high frequency output voltage and current of the receiver. R_L is the equivalent load resistance.

The equivalent circuit of LCL-S compensated wireless charging system is shown in Fig. 2.

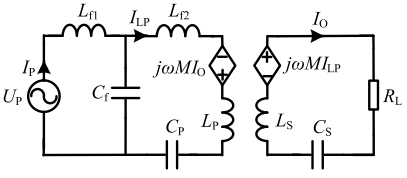

FIGURE 2. Equivalent circuit of LCL-S compensated wireless charging system.

According to the Kirchhoff Voltage Law (KVL), the equations of loops in Fig. 2 are shown in (1).

$$\begin{cases} U_P = I_P(j\omega L_{f1}) + (I_P - I_{LP})(\dfrac{1}{j\omega C_f}) \\ 0 = -(I_P - I_{LP})(\dfrac{1}{j\omega C_f}) \\ \qquad + I_{LP}(j\omega L_{f2} + j\omega L_P + \dfrac{1}{j\omega C_P}) - j\omega MI_O \\ 0 = -j\omega MI_{LP} + I_O(j\omega L_S + \dfrac{1}{j\omega C_S} + R_L) \end{cases} \tag{1}$$

In order to keep the system in resonance, the resonant frequency of the primary side should be the same as the secondary side, $\omega_{sr} = \omega_{pr} = \omega$. And when $L_{f1} = L_{f2}$, the current in the transmitting coil can keep constant [10]. Therefore, the relation equations can be presented as (2).

$$\begin{cases} j\omega L_{f1} = j\omega L_{f2} = -\dfrac{1}{j\omega C_f} \\ j\omega L_P = -\dfrac{1}{j\omega C_P} \\ j\omega L_S = -\dfrac{1}{j\omega C_S} \end{cases} \tag{2}$$

Setting $L_{f1} = L_{f2} = L_f$ and substituting (2) into (1), the solution of loop current can be obtained as (3).

$$\begin{cases} I_P = \dfrac{M^2 U_P}{L_f^2 R_L} \\ I_{LP} = \dfrac{U_P}{j\omega L_f} \\ I_O = \dfrac{M U_P}{L_f R_L} \end{cases} \tag{3}$$

The voltage or current gain of the system can be derived as shown in (4).

$$\begin{cases} G_{UU} = \dfrac{U_O}{U_P} = \dfrac{I_O R_L}{U_P} = \dfrac{M}{L_f} \\ G_{UI} = \dfrac{I_O}{U_P} = \dfrac{M}{L_f R_L} \\ G_{IU} = \dfrac{U_O}{I_P} = \dfrac{I_O R_L}{I_P} = \dfrac{M}{L_f} \\ G_{II} = \dfrac{I_O}{I_P} = \dfrac{L_f}{M R_L} \end{cases} \tag{4}$$

Therefore, the output voltage U_O of the charging system $U_O = G_{UU} U_P = M U_P / L_f$, and the current in the transmitting coil $I_{LP} = U_P / j\omega L_f$ are both independent with load.

Moreover, the total input impedance can be derived as shown in (5), and it can be seen that the total input impedance only has the real parts and therefore the system with LCL-S compensation topology can realize ZPA.

$$Z_T = \frac{U_P}{I_P} = \frac{L_f^2 R_L}{M^2} \tag{5}$$

Results obtained from derivations show that wireless charging system with LCL-S compensation topology can achieve CV output for batteries and the current in the transmitting coil is stable even with misalignment.

B. ANALYSIS OF LCL-LCL COMPENSATION TOPOLOGY

Stable load-independent CV output can be achieved with LCL-S compensation topology according to the above analysis. The purpose of this Section is to analyze the compensation topology with CC output. And the topology scheme of the LCL-LCL compensated wireless charging system is shown in Fig. 3. L_{g1}, L_{g2} and C_g are the resonant elements of LCL compensation topology at the receiver side. The meanings of other symbols are the same as those in Section *A*.

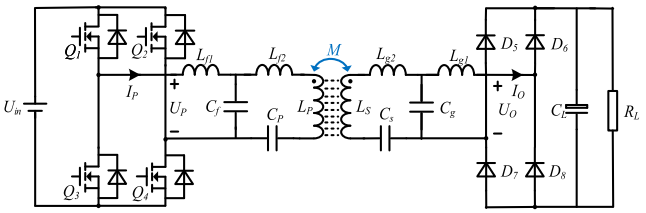

FIGURE 3. Converter circuit of LCL-LCL compensated wireless charging system.

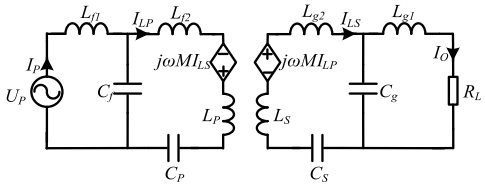

FIGURE 4. Equivalent circuit of LCL-LCL compensated wireless charging system.

The equivalent circuit of LCL-LCL compensated wireless charging system is shown in Fig. 4.

According to the Kirchhoff Voltage Law (KVL), the equations of loops in Fig. 4 are shown in (6).

$$\begin{cases} U_P = I_P(j\omega L_{f1}) + (I_P - I_{LP})(\dfrac{1}{j\omega C_f}) \\ 0 = -(I_P - I_{LP})(\dfrac{1}{j\omega C_f}) \\ \qquad + I_{LP}(j\omega L_{f2} + j\omega L_P + \dfrac{1}{j\omega C_P}) - j\omega M I_O \\ 0 = -j\omega M I_{LP} + I_{LS}(j\omega L_{g2} + j\omega L_S + \dfrac{1}{j\omega C_S}) \\ \qquad + (I_{LS} - I_O)(\dfrac{1}{j\omega C_g}) \\ 0 = -(I_{LS} - I_O)(\dfrac{1}{j\omega C_g}) + I_O(j\omega L_{g1} + R_L) \end{cases} \tag{6}$$

In order to keep system in resonant state, the resonant frequency of the primary side should be the same as the secondary side, $\omega_{sr} = \omega_{pr} = \omega$. When $L_{f1} = L_{f2}$ and $L_{g1} = L_{g2}$, the topology can realize constant current characteristic [10]. Therefore, the relation presented can be derived as (7).

$$\begin{cases} j\omega L_{f1} = j\omega L_{f2} = -\dfrac{1}{j\omega C_f} \\ j\omega L_{g1} = j\omega L_{g2} = -\dfrac{1}{j\omega C_g} \\ j\omega L_P = -\dfrac{1}{j\omega C_P} \\ j\omega L_S = -\dfrac{1}{j\omega C_S} \end{cases} \tag{7}$$

Setting $L_{f1} = L_{f2} = L_f$, $L_{g1} = L_{g2} = L_g$ and substituting (7) into (6), the solution of loop current can be obtained

as (8).

$$\begin{cases} I_{\mathrm{P}} = \dfrac{M^2 U_P R_L}{\omega^2 L_f^2 L_g^2} \\ I_{\mathrm{LP}} = \dfrac{U_P}{j\omega L_f} \\ I_{\mathrm{LS}} = \dfrac{M U_P R_L}{\omega^2 L_f L_g^2} \\ I_{\mathrm{O}} = \dfrac{M U_P}{j\omega L_f L_g} \end{cases} \tag{8}$$

The voltage or current gain of the system can be derived as shown in (9).

$$\begin{cases} G_{UU} = \dfrac{U_O}{U_P} = \dfrac{I_O R_{\mathrm{L}}}{U_P} = \dfrac{M R_{\mathrm{L}}}{j\omega L_{\mathrm{f}} L_{\mathrm{g}}} \\ G_{UI} = \dfrac{I_O}{U_P} = \dfrac{M}{j\omega L_{\mathrm{f}} L_{\mathrm{g}}} \\ G_{IU} = \dfrac{U_O}{I_P} = \dfrac{I_O R_L}{I_P} = \dfrac{\omega L_f L_g}{jM} \\ G_{II} = \dfrac{I_O}{I_P} = \dfrac{\omega L_f L_g}{jMR_L} \end{cases} \tag{9}$$

Therefore, the output current I_{O} of the charging system $I_O = G_{UI} U_P = M_{UP}/j\omega L_P$, and the current in the transmitting coil $I_{LP} = U_P/j\omega L_P$ are both load-independent.

Moreover, the total input impedance can be derived as shown in (10), and it can be seen that the total input impedance does not contain imaginary parts and the system with LCL-LCL compensation topology can realize ZPA.

$$Z_{\mathrm{T}} = \frac{U_P}{I_P} = \frac{\omega^2 L_f^2 L_g^2}{M^2 R_L} \tag{10}$$

Conclusions can be drawn based on results obtained from the derivations that the charging system with LCL-LCL compensation topology can achieve CV output for batteries, and it can realize ZPA. It is worth mentioning that other compensation mode such as parallel (P) connection in receiver and LCL in transmitter can achieve CV output, but the total input impedance contains imaginary parts [10].

III. DESIGN OF COMPENSATION TOPOLOGY

As analyzed above, the LCL-S compensated wireless charging system can achieve CV output and the LCL-LCL compensated wireless charging system can achieve CC output, both can realize ZPA. It is reasonable to think that CV/CC output can be implemented by combination of these two topologies. The resonant element of LCL compensation topology L_{f2} or L_{g2} can be equivalent into the self-inductance of the coil as shown in Fig. 5. And C_P' can be drawn from (11) and shown in (12).

$$j\omega L_{f2} + j\omega L_P + \frac{1}{j\omega C_P} = j\omega L_P + \frac{1}{j\omega C_P'} \tag{11}$$

$$C_P' = \frac{1}{\omega^2 (L_P - L_f)} \tag{12}$$

Consequently, the designed topology scheme that includes LCL compensation in transmitter and LCL or S switching

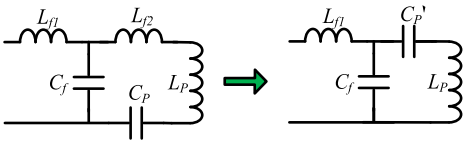

FIGURE 5. Simplified resonant element of LCL compensation topology.

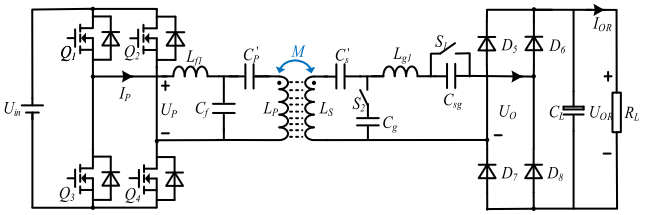

FIGURE 6. Converter circuit of LCL-S/LCL switching compensated wireless charging system.

compensation in receiver is shown in Fig. 6, which can realize a stable CC/CV output.

In Fig. 6, when switches S_1 and S_2 are disconnected, the system achieves CV output. And when switches S_1 and S_2 are turned on, the system achieves CC output. The additional switches S_1 and S_2 are constructed with two anti-series connected MOSFETs. The total impendence of C_S', L_{g1} and C_{sg} is equal to $j\omega C_S$ when S_1 and S_2 are disconnected, thus the added capacitor C_{sg} can be calculated as (13).

$$C_{sg} = \frac{1}{2\omega^2 L_g} \tag{13}$$

The impact of the switching state on the system stability should be concerned. The current in the transmitting coil before and after switching can be represented as (14).

$$I_{LP-B} = I_{LP-F} = \frac{U_P}{j\omega L_f} \tag{14}$$

It can be seen that the current in the transmitting coil is stable when U_P is fixed before and after switching. The voltage gain and current gain of the system with dynamic LCL-S/LCL switching topology shown in Fig. 6 can be derived as (15).

$$\begin{cases} G_{UU} = \dfrac{U_O}{U_P} = \dfrac{I_O R_{\mathrm{L}}}{U_P} = \dfrac{M}{L_{\mathrm{f}}} \\ G_{UI} = \dfrac{I_O}{U_P} = \dfrac{M}{j\omega L_f L_g} \end{cases} \tag{15}$$

Based on the analysis of dynamic LCL-S/LCL switching topology, the design flow of the dynamic compensated wireless charging system is shown in Fig. 7. Firstly, according to the given dimension and electrical parameters of the charging system for the applied EVs, the coupling structure is designed based on section III. Then equivalent circuit parameters of the coupling structure can be measured. Further, the voltage gain G_{UU} and current gain G_{UI} of the system are calculated based on the desired voltage and current output. L_f and L_g can be changed to regulate the voltage or current gain of the system based on (15). Finally, other capacitance values of the system can be obtained based on the related equations.

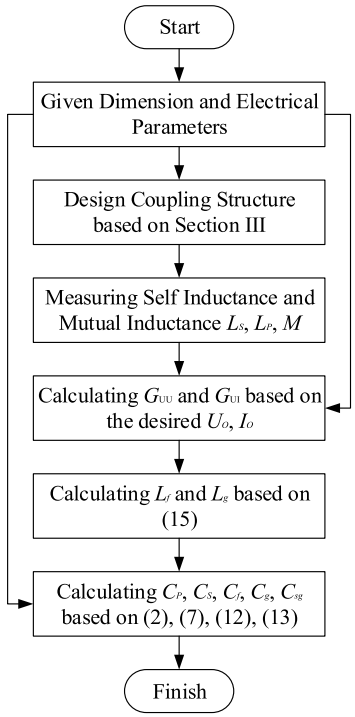

FIGURE 7. Design flow of the dynamic compensation wireless charging system.

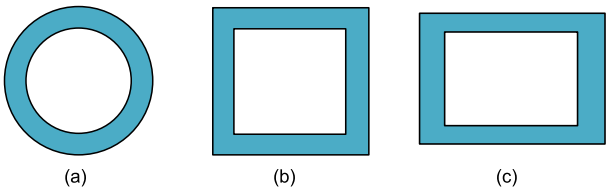

FIGURE 8. Conventional coil structure. (a) Circular coil. (b) Square coil. (c) Rectangular coil.

IV. DESIGN AND OPTIMIZATION OF COUPLING STRUCTURE

A. COIL STRUCTURE

Generally, circular, square and rectangular coil structure are used in wireless charging system as shown in Fig. 8, and the former two type coils are often adopted to make coupling structure expansion easier [19], [20]. The key to coupling structure design is the layout of quality factor and coupling coefficient [12]. And coupling factor k is shown in (16) and quality factor Q of coupling coil is shown in (17).

$$k = \frac{M}{\sqrt{L_P L_S}} = \frac{M_0 n_P n_S}{\sqrt{n_P^2 L_{P0} n_S^2 L_{S0}}} = \frac{M_0}{\sqrt{L_{P0} L_{S0}}} \tag{16}$$

$$Q = \frac{\omega L}{R} \tag{17}$$

L_{P0}, L_{S0}, M_{S0} are the self-inductance and mutual inductance of single turn coil and n_P, n_S is turns number of the transmitting and receiving coils in (16) and (17). In order to obtain coupling performance difference between circular and square coupling coils, equivalent inductance values of these

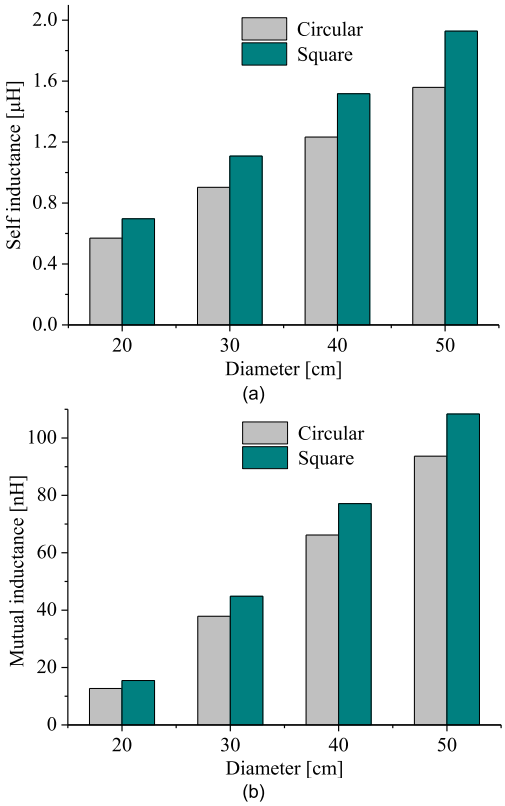

FIGURE 9. Equivalent inductance of two different coil structures with diameters changing. (a) Self-inductance. (b) Mutual-inductance.

two coil structures with only one-turn are compared under four coil diameters (20 cm, 30 cm, 40 cm, 50 cm) and the results are shown in Fig. 9.

From the results in Fig. 9, it can be seen that square coil structure has greater self-inductance and mutual-inductance than circular coil with same diameter.

A certain horizontal offset of coupling coils may occur due to the imperfect parking of EVs. Therefore, the mutual inductances of the two structures under different horizontal offsets are compared. The coupling change rate Δk_t shown in (18) is defined to indicate the stability of coupling. And smaller coupling change rate means better coupling stability.

$$\Delta k_t = \frac{k_{t-\Delta t} - k_t}{\Delta t} \tag{18}$$

Therefore, the coupling change rates of the two structures with the same diameter of 40 cm under different offsets are computed and shown in Fig. 10.

From the results in Fig. 10, it can be seen that the mutual inductance of square coils keeps more stable and changes more slowly when horizontal offset happens. At the same time, the current at the right angle of square coil is uneven due to skin effect and proximity effect and fillet design can be adopted to avoid the effect at the corner of square coil to reduce resistance losses. Therefore, square coil structure with rounded corners is adopted to construct coupling structure to achieve stable coupling performance and loss reduction in this paper.

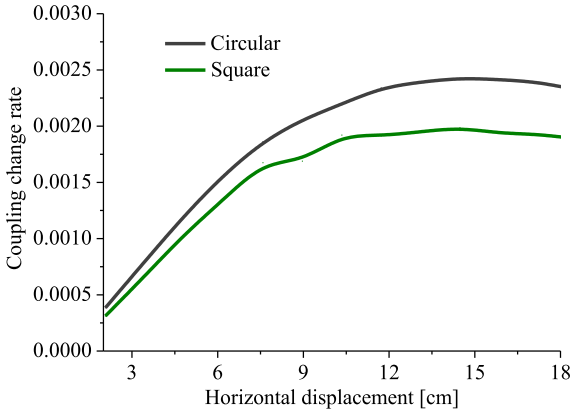

FIGURE 10. Coupling change rate of two coil structures with displacement changing.

Without considering the switch loss of the wireless charging system and the transmitting and receiving coils are regarded as the same, the transmission efficiency of the system in Fig. 2 is shown as:

$$\eta = \frac{k^2 Q_P Q_{SL}}{1 + k^2 Q_P Q_{SL}} \cdot \frac{Q_{SL}}{Q_L} \tag{19}$$

Where $Q_P = \omega L_P / R_P$, $Q_S = \omega L_S / R_S$, $Q_L = \omega L_S / R_L$, $Q_{SL} = Q_S Q_L / (Q_S + Q_L)$.

Setting $d\eta / dQ_L = 0$, the optimal Q_L value can be obtained:

$$Q_L = \frac{Q_S}{(1 + k^2 Q_P Q_S)^{1/2}} \tag{20}$$

Figure-of-Merit (*FOM*) is defined to evaluate the performance of the system and $FOM = kQ$. Thus, the transmission efficiency of the system with optimized load is shown as:

$$\eta_{Load-opt} = \frac{FOM^2}{4(1 + FOM^2)^{1/2} + 2FOM^2} \tag{21}$$

Thus, the *FOM* in (21) is converted to the geometric parameters to guide the design of coil parameters as shown in (22).

$$FOM^2 = \frac{2\pi^2 \mu_0 \omega \sigma N^2 a^2 r^6}{D^6} \tag{22}$$

μ_0 is vacuum permeability, μ_r is relative permeability, r is the coil radius, N is the number of coil turns, D is the transmission distance, a is the wire diameter, σ is the wire conductivity, ω is the system angular frequency. Setting $A = 2\pi^2 \mu_0 \omega \sigma N^2 a^2 r^6$ in (22), the (21) can be reduced to (23).

$$\eta_{load-opt} = \frac{\frac{A}{D^6}\sqrt{\frac{A}{D^6} + 1}}{\left(\frac{A}{D^6} + 1 + \sqrt{\frac{A}{D^6} + 1}\right)\left(\sqrt{\frac{A}{D^6} + 1} + 1\right)} \tag{23}$$

According to (23), the relation among the transmission efficiency η, the size parameter A and the transmission distance D can obtained and shown in Fig. 11.

The maximum occupied area is about 1600 cm^2 and the transmission distance is about 15 cm according to operation conditions for the designed wireless charging system in this paper. And the desired resonant frequency is 100 kHz. According to the actual application conditions and relation among the transmission efficiency η, the size parameter A and the transmission distance D, the designed coil with 40 cm diameter and 12 turns is shown in Fig. 12.

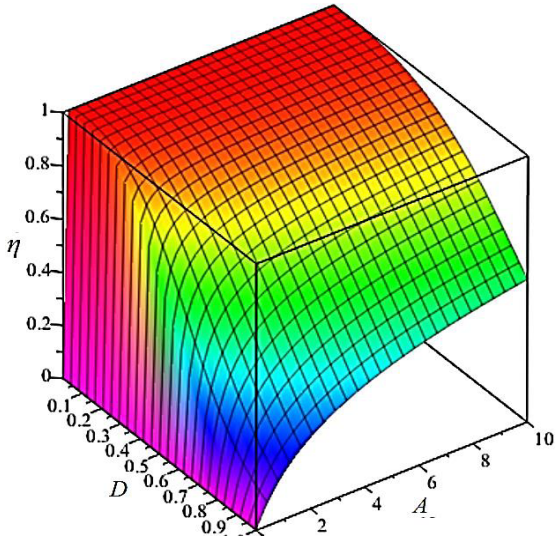

FIGURE 11. Relation among transmission efficiency η, size parameter *A* and transmission distance *D*.

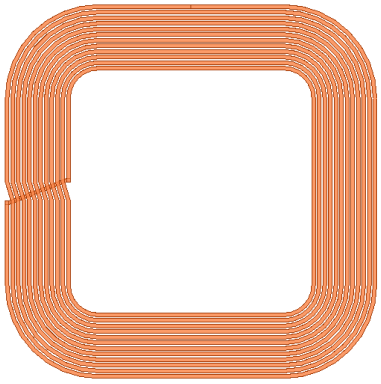

FIGURE 12. The designed coil structure.

B. SHIELDING STRUCTURE

Magnetic shielding structure can be added to enhance the coupling performance between transmitting coil and receiving coil and reduce the leakage of magnetic field [5]. The magnetic shielding usually consists of magnetic medium with high relative permeability (magnetic core) in the resonant magnetic circuit. Magnetic cores with a relatively larger transmission area are generally used to lay out the side of the coil in a certain way. Depending on the layout mode of magnetic core, this paper sets up four different shielding structures ***B***, ***C***, ***D*** and ***E***, as shown in Fig. 13 (b) - (e), ***B*** with flat magnetic core, ***C*** with "E" type magnetic core, ***D*** with hollow stripe magnetic core extended from the flat magnetic core, ***E*** with splicing magnet core units according to the needs of installing.

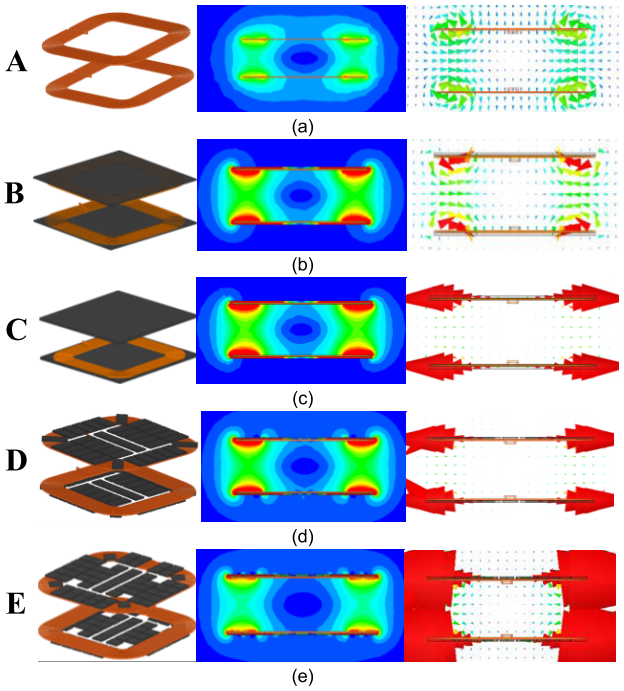

FIGURE 13. The coupling structure with different shielding structures, the amplitude distribution of magnetic induction intensity, and vector distribution of magnetic induction intensity. (a) *A*-without magnetic cores. (b) *B*-with flat magnetic core. (c) *C*- with "E" type magnetic core. (d) *D*- with hollow stripe magnetic core. (e) E- with splicing magnet core units.

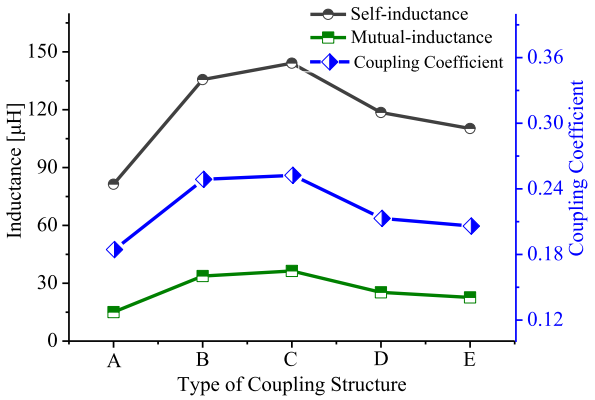

FIGURE 14. Equivalent circuit parameter of five type coupling structures.

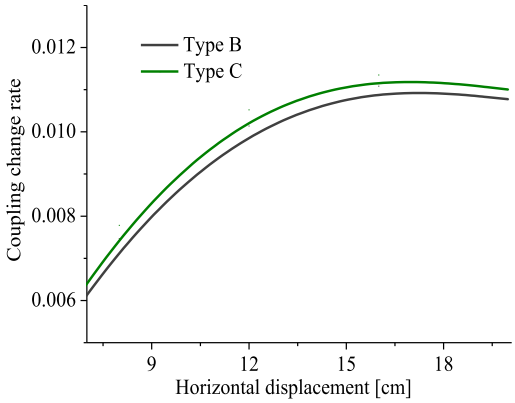

FIGURE 15. Coupling change rate of type *B* and *C* structure with horizontal displacement changing.

In Fig. 13, ***A*** is a coupling structure without magnetic shielding structure, ***B***-***E*** are coupling structures with four different magnetic core layout schemes, and corresponding amplitude distribution of magnetic induction intensity and vector distribution of magnetic induction intensity. According to amplitude and vector distribution of magnetic induction intensity, most magnetic flow of coupling structure without shielding structure passes through the transmitting and receiving coils, but there are still some magnetic lines forming a closed loop through the air; coupling structure with ***B*** type shielding structure constrains the distribution of magnetic field and the magnetic flows are concentrated along the direction of the magnetic core placement which means the coupling performance has been improved; coupling structure with ***C*** type shielding structure also improves the magnetic flows through the transmitting and receiving coils; coupling structure with ***D*** type shielding structure has almost the same magnetic field restriction capacity as ***B*** structure, while saving nearly 1/3 weight of the magnetic core; magnetic field binding ability of coupling structure with ***E*** type shielding structure is similar to ***D***, however, ***E*** type shielding structure consists of block magnetic core splicing and it is convenient for manufacture and installation.

Equivalent circuit parameters of the above five coupling structures with different shielding structure from simulation results are shown in Fig. 14. The coupling structure with ***C*** type shielding structure has the highest self-inductance, mutual-inductance and coupling coefficient. But another key factor is the coupling stability when horizontal displacement happens because of parking deviation and uneven misalignment of EVs. Therefore, the coupling change rate of coupling structures with plate magnetic core and "E" type magnetic core is computed and shown in Fig. 15. It can be seen that coupling structures with ***B*** plate magnetic core has a certain better position fault tolerance range compared with "E" type magnetic core. The structure with plate magnetic core is more suitable for the wireless charging system of EVs.

Coupling structure with ***E*** type shielding structure is simplified from type ***B*** for manufacture and installation convenience. And it has almost the same equivalent circuit coupling parameters with structure ***B*** but with more than 1/3 weight saving and cost reduction of the magnetic core. Therefore, the coupling coil with type E shielding structure is selected as the system's transmitting and receiving coupling structures according to actual demand. The designed unsealed coupling structure is shown in Fig. 16.

V. EXPERIMENT

According to the structure designed in Section IV, the coupling structure is manufactured as shown in Fig. 17. And the measured equivalent parameters of the manufactured

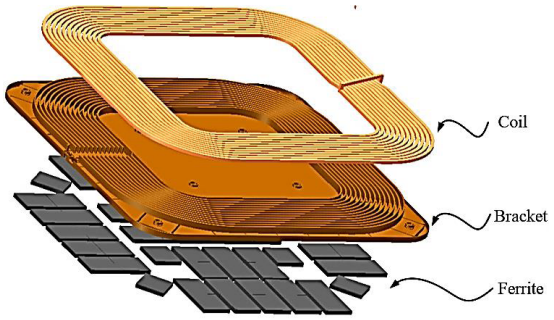

FIGURE 16. The designed coupling structure.

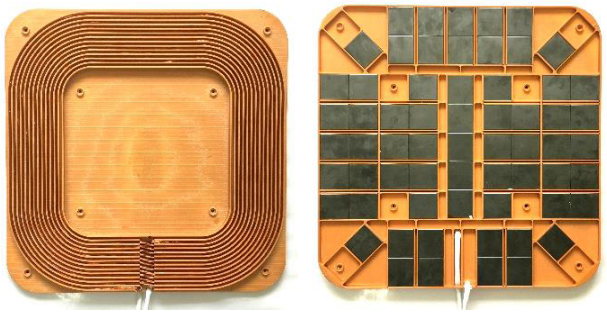

FIGURE 17. The manufactured coupling structure. (a) Coil of coupling structure. (b) Shielding of coupling structure.

FIGURE 18. Equivalent parameters of the manufactured coupling structure.

coupling structure are shown in Fig. 18. The equivalent self-inductance of the coupling structure is 107.492 μH and the quality factor is 352 under 100 kHz with the mutual-inductance of 17.9 uH.

The desired output voltage and current for battery charging is 144 V and 9 A respectively. Based on design flow shown in Fig. 8, the parameters of compensation circuit elements can be computed and given in Table 1. The wireless charging system with these parameters is established as in Fig. 19.

TABLE 1. Parameters of compensation circuit elements.

L_{f1}	C_f	C_p'	C_s'	C_g	C_{sg}	L_{g1}
30 μH	84.4 nF	32.7 nF	29 nF	126 nF	63.2 nF	20 μH

The performance of current in transmitting coil and CV/CC output characteristic with varied load is tested and shown in the following. Fig. 20 shows the measured waveforms when switches S_1 and S_2 are disconnected. It could be clearly seen that the output voltage U_{OR} is constant about 144 V with load changing from 14.5 Ω to 9.5 Ω in Fig. 20(b). And the

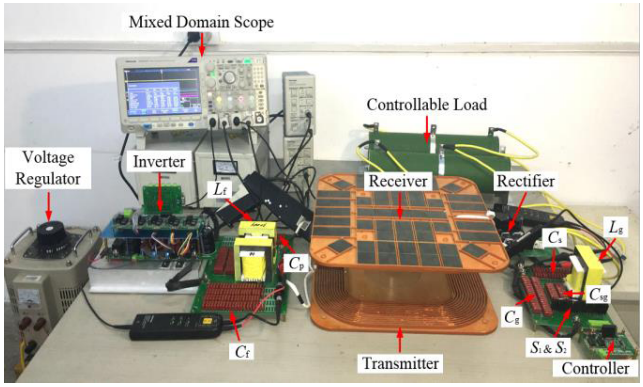

FIGURE 19. The established resonant wireless charging system.

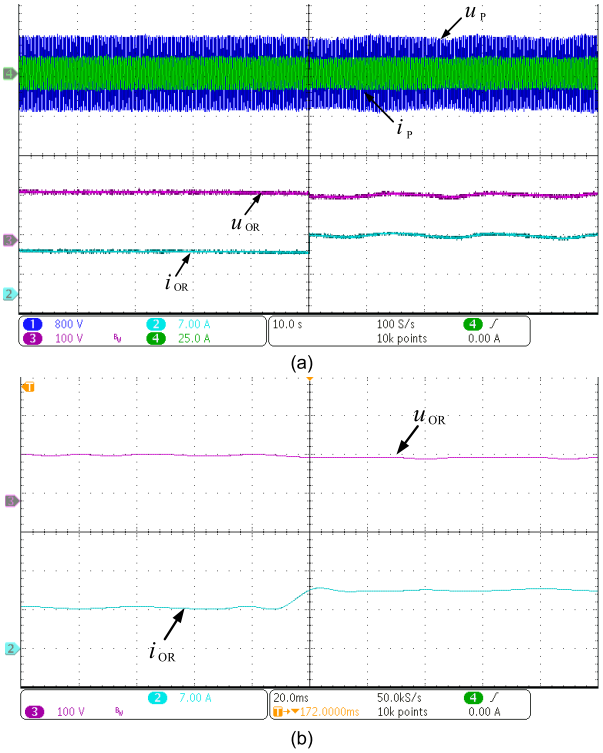

FIGURE 20. The measured waveforms in CV output mode when load changes from 14.5Ω to 9.5Ω. (a) Waveforms of u_p, i_p, u_{or} and i_{or}. (b) Waveforms of u_{or} and i_{or}.

tiny fluctuations of output voltage at the switching moment are considered to be caused by the corresponding parasitic resistance and the nonideal experimental device.

Fig. 21 shows the measured waveforms when switches S_1 and S_2 are closed. It is clearly seen that the output current I_{OR} is constant with load changing from 14.5 Ω to 9.5 Ω in Fig. 21 (b).

According to the waveforms in Fig. 20 (a) and Fig. 21 (a), it can be obtained that the current in transmitting coil is independent from load variance. And the experiment results also present that the implemented system achieves CV output and CC output with varied load, which is consistent with analytical design.

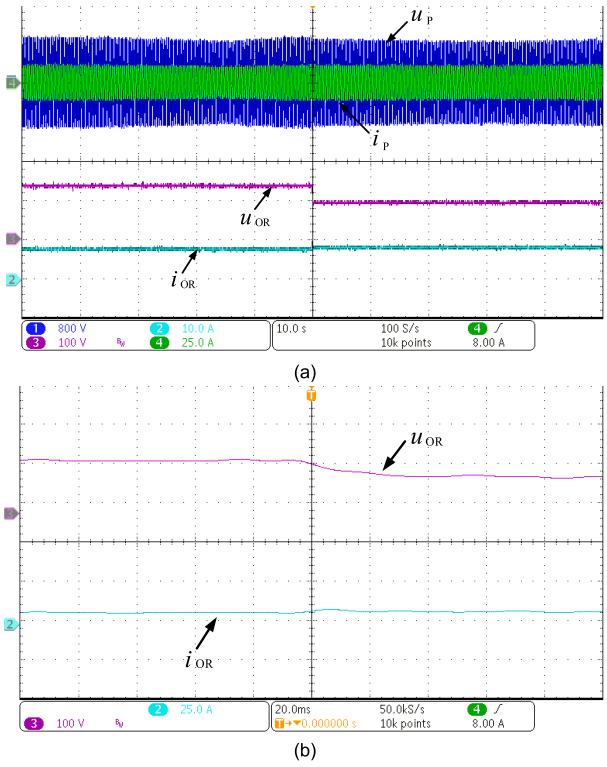

FIGURE 21. The measured waveforms in CC output mode when load changes from 14.5 Ω to 9.5 Ω. (a) Waveforms of u_p, i_p, u_{or} and i_{or}. (b) Waveforms of u_{or} and i_{or}.

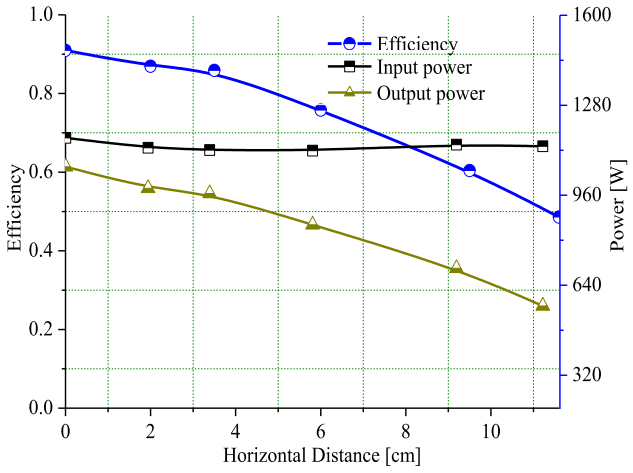

FIGURE 22. Transmission efficiency versus horizontal distance.

Moreover, the transmission efficiency versus horizontal displacement of the implemented system in CV mode is tested and shown in Fig. 22.

The overall efficiency presents the same stable trend as simulation results. And when the horizontal offset ranges from −5 cm to 5 cm, the system efficiency only decreases by ten percent. And the system with well-faced coupling can achieve 1297.69 W output power with efficiency of 90.94%.

VI. CONCLUSION

LCL compensation topology in the transmitter can make the current constant in the transmitting coil even if the reflected impedance of receiver changes due to the parking deviation and misalignment of EVs. LCL-S compensated wireless charging system can achieve CV output and the LCL-LCL compensated wireless charging system can achieve CC output, both of which can realize ZPA. The designed topology scheme that includes LCL compensation in transmitter and LCL or S switching compensation in receiver can realize constant current in the transmitting coil and CC/CV output. Moreover, additional compensation inductance of LCL topology can be adjusted to regulate the voltage or current gain of the system.

Square coil structure with the same diameter has greater self-inductance and mutual-inductance than circular coil structure. And the mutual inductance of square coil keeps more stable when horizontal offset happens. At the same time, coupling structures with plate magnetic core has a certain range of position fault tolerance compared to "E" type magnetic core. The structure with plate magnetic core is more suitable for the wireless EVs charging system. Therefore, rounded rectangular spiral coil and splicing magnet core units are adopted to the construct coupling structure of wireless EVs charging to achieve a stable coupling performance and loss reduction.

Finally, the resonant wireless charging system for EVs is built and tested according to the design and optimization of dynamic compensation topology and its coupling structure. The experimental results show that the system's load-independent and other characteristics are well correlated with the theoretical analysis. The efficiency of the designed system with 12.5% horizontal offset decreases only less than 10%, and output power of the well-faced system can reaches 1297.69 W with the efficiency of 90.94%.

REFERENCES

[1] A. Kurs, A. Karalis, R. Moffatt, J. D. Joannopoulos, P. Fisher, and M. Soljačić, "Wireless power transfer via strongly coupled magnetic resonances," *Science*, vol. 317, no. 5834, pp. 83–86, Jul. 2007, doi: 10.1126/science.1143254.

[2] D. Kurschner, C. Rathge, and U. Jumar, "Design methodology for high efficient inductive power transfer systems with high coil positioning flexibility," *IEEE Trans. Ind. Electron.*, vol. 60, no. 1, pp. 372–381, Jan. 2013, doi: 10.1109/TIE.2011.2181134.

[3] A. P. Sample, D. T. Meyer, and J. R. Smith, "Analysis, experimental results, and range adaptation of magnetically coupled resonators for wireless power transfer," *IEEE Trans. Ind. Electron.*, vol. 58, no. 2, pp. 544–554, Feb. 2011, doi: 10.1109/TIE.2010.2046002.

[4] J. Wang, C. Cai, M. Long, K. Liu, and M. Sun, "Study of resonant self-charging rats experiment playground based on Witricity technology," *Int. J. Appl. Electromagn. Mech.*, vol. 53, no. 3, pp. 409–421, Feb. 2017, doi: 10.3233/JAE-160054.

[5] F. Musavi and W. Eberle, "Overview of wireless power transfer technologies for electric vehicle battery charging," *IET Power Electron.*, vol. 7, no. 1, pp. 60–66, Jan. 2014, doi: 10.1049/iet-pel.2013.0047.

[6] T. Mizuno, S. Yachi, A. Kamiya, and D. Yamamoto, "Improvement in efficiency of wireless power transfer of magnetic resonant coupling using magnetoplated wire," *IEEE Trans. Magn.*, vol. 47, no. 10, pp. 4445–4448, Oct. 2011, doi: 10.1109/TMAG.2011.2158525.

[7] H.-J. Song, H. Shin, H.-B. Lee, J.-H. Yoon, and J.-K. Byun, "Induced current calculation in detailed 3-D adult and child model for the wireless power transfer frequency range," *IEEE Trans. Magn.*, vol. 50, no. 2, pp. 1041–1044, Feb. 2014, doi: 10.1109/TMAG.2013.2282364.

[8] A.-H. Hussein and I. Batarseh, "A review of charging algorithms for nickel and lithium battery chargers," *IEEE Trans. Veh. Technol.*, vol. 60, no. 3, pp. 830–838, Mar. 2011, doi: 10.1109/TVT.2011.2106527.

[9] M. D. Yin, J. Youn, D. Park, and J. Cho, "Dynamic frequency and duty cycle control method for fast pulse-charging of lithium battery based on polarization curve," in *Proc. Int. Conf. Frontier Comput. Sci. Technol.*, Aug. 2015, pp. 40–45, doi: 10.1109/FCST.2015.33.

[10] H. Hao, G. A. Covic, and J. T. Boys, "An approximate dynamic model of LCL-*T*-based inductive power transfer power supplies," *IEEE Trans. Power Electron.*, vol. 29, no. 10, pp. 5554–5567, Oct. 2014, doi: 10.1109/TPEL.2013.2293138.

[11] Y. Song, U. K. Madawala, D. J. Thrimawithana, and A. P. Hu, "LCL and CL compensations for wireless three phase bi-directional EV charging systems," in *Proc. Power Electron. Conf.*, Dec. 2017, pp. 1–6.

[12] R. Bosshard, J. Mühlethaler, J. W. Kolar, and I. Stevanović, "Optimized magnetic design for inductive power transfer coils," in *Proc. Appl. Power Electron. Conf. Expo.*, Mar. 2013, pp. 1812–1819.

[13] M. Budhia, G. A. Covic, and J. T. Boys, "Design and optimization of circular magnetic structures for lumped inductive power transfer systems," *IEEE Trans. Power Electron.*, vol. 26, no. 11, pp. 3096–3108, Nov. 2011, doi: 10.1109/TPEL.2011.2143730.

[14] Y. Liu, S. Bai, W. Zhang, and K. Li, "Design and optimization of mutual inductance for high efficiency ICPT system," in *Proc. IEEE Int. Power Electron. Motion Control Conf.*, May 2016, pp. 3178–3182.

[15] T.-D. Yeo, D. Kwon, S.-T. Khang, and J.-W. Yu, "Design of maximum efficiency tracking control scheme for closed-loop wireless power charging system employing series resonant tank," *IEEE Trans. Power Electron.*, vol. 32, no. 1, pp. 471–478, Jan. 2016, doi: 10.1109/TPEL.2016.2523121.

[16] S. Kai, L. Zhenjie, D. Zhijiang, and Z. Chunbo, "Constant current charging technology for variable load wireless charging system," *Trans. China Electrotechn. Soc.*, vol. 32, no. 13, pp. 130–136, Jul. 2017, doi: 10.19595/j.cnki.1000-6753.tces.161156.

[17] W. Zhang, S.-C. Wong, C. K. Tse, and Q. Chen, "Load-independent duality of current and voltage outputs of a series- or parallel-compensated inductive power transfer converter with optimized efficiency," *IEEE J. Emerg. Sel. Topics Power Electron.*, vol. 3, no. 1, pp. 137–146, Mar. 2015, doi: 10.1109/JESTPE.2014.2348558.

[18] X. Qu, H. Han, S. C. Wong, C. K. Tse, and W. Chen, "Hybrid IPT topologies with constant current or constant voltage output for battery charging applications," *IEEE Trans. Power Electron.*, vol. 30, no. 11, pp. 6329–6337, Nov. 2015, doi: 10.1109/TPEL.2015.2396471.

[19] M. Budhia, J. T. Boys, G. A. Covic, and C.-Y. Huang, "Development of a single-sided flux magnetic coupler for electric vehicle IPT charging systems," *IEEE Trans. Ind. Electron.*, vol. 60, no. 1, pp. 318–328, Jan. 2013, doi: 10.1109/TIE.2011.2179274.

[20] M. Kiani, U.-M. Jow, and M. Ghovanloo, "Design and optimization of a 3-coil inductive link for efficient wireless power transmission," *IEEE Trans. Biomed. Circuits Syst.*, vol. 5, no. 6, pp. 579–591, Dec. 2011, doi: 10.1109/TBCAS.2011.2158431.

CHANGSONG CAI was born in Henan, China, in 1992. He received the B.S. degree in electrical engineering from Tianjin Polytechnic University, Tianjin, China, in 2014 and the M.Eng. degree in electrical engineering from Wuhan University, Wuhan, China, in 2017, where he is currently pursuing the Ph.D. degree in electrical engineering.

His current research interests include applied electromagnetics and power electronics, the research mainly involves wireless power transfer based on magnetic resonance and its industrial applications.

JUNHUA WANG was born in Shandong, China, in 1981. He received the Ph.D. degree from The Hong Kong Polytechnic University, Hong Kong, in 2012. He is currently a Professor with the School of Electrical Engineering, Wuhan University.

He joined Carnegie Mellon University as a Post-Doctoral Researcher in 2012 and then a Research Fellow at GATE Center for Electric Drive Transportation, Michigan, USA.

His main research interests include wireless transfer technology based on magnetic resonance, applied electromagnetics, system equipment for power transmission, and distribution.

ZHIJIAN FANG received the B.S. and Ph.D. degrees in electrical engineering and automation from the Huazhong University of Science and Technology, Wuhan, China, in 2010 and 2015, respectively.

Since 2015, he has been a Post-Doctoral Research Fellow with the School of Electrical Engineering, Wuhan University, Wuhan, China. From 2016 to 2017, he was a Post-Doctoral Research Fellow with the Department of Electrical and Computer Engineering, Ryerson University, Toronto, Canada.

His research interests include high performance dc/dc converter, battery charger, and renewable energy applications.

PENGCHENG ZHANG was born in Anhui, China, in 1991. He received the B.S. degree in electrical engineering and the M.S. degree in control science and engineering from Tianjin Polytechnic University, Tianjin, China, in 2013 and 2016, respectively. He is currently pursuing the Ph.D. degree with the Hebei University of Technology, Tianjin.

Since 2017, he has been a Visiting Researcher with the School of Electrical and Computer Engineering, Georgia Institute of Technology, Atlanta, GA, USA.

His main research interests include wireless power transfer based on magnetic resonance and its applications in EV charging.

MEILIN HU was born in Hubei, China, in 1994. She received the B.S. degree in electrical engineering from Wuhan University, Wuhan, China, in 2016, where she is currently pursuing the M.S. degree in electrical engineering with the School of Electrical Engineering.

Her main research interests include design and optimization and of wireless power transfer system based on resonant magnetic coupling, electromagnetic environment, and security evaluation for wireless charging.

JUNKUN ZHANG was born in Hubei, China, in 1992. He received the M.S. degree in power electronics and power transmission from the Wuhan University of Technology. He is currently an Assistant Engineer with the Institute of New Energy, Wuhan.

His main research interests include wireless power transfer based on magnetic resonance and its applications in EV charging.

LIANG LI was born in Jiangxi, China, in 1996. He received the B.S. degree in engineering from the College of Hydropower and Digital Engineering, Huazhong University of Science and Technology, in 2017. He is currently pursuing the M.S. degree in electrical engineering with the School of Electrical Engineering, Wuhan University.

His main research interests include wireless power transfer based on magnetic resonance and its applications in EV charging.

ZHONGZHENG LIN was born in Fujian, China, in 1993. He received the B.S. degree in electrical engineering from Wuhan University, China, in 2017, where he is currently pursuing the M.S. degree in electrical engineering with the School of Electrical Engineering.

His current research interests include wireless power transfer and power electronics, the research mainly involves the magnetic resonance coupling theory, the application research, and the dynamic charging technology research.